에너지공학, 제23권 제4호(2014)
Journal of Energy Engineering, Vol. 23, No. 4, pp.73~87(2014)
http://dx.doi.org/10.5855/ENERGY.2014.23.4.073

An Overall Investigation of Break Simulators for LOCA Scenarios in Integral Effect Tests

Yeon-Sik Kim† and Hyun-Sik Park
Korea Atomic Energy Research Institute
(Received 29 August 2014, Revised 1 December 2014, Accepted 4 December 2014)

Abstract

Various studies on the critical flow models for sub-cooled and/or saturated water were reviewed, especially on Fauske, Moody, and Henry for basic theoretical models; Zaloudek for insight into physical phenomena for a critical flow in an orifice type flow path; Sozzi & Sutherland for a critical flow test of saturated and sub-cooled water at high pressure for orifice and nozzles; and a Marviken test on a full-scale critical flow test. In addition, critical flow tests of sub-cooled water for the break simulators in integral effect test (IET) facilities were also investigated, and a hybrid concept using Moody's and Fauske's models was considered by the authors. In the comparison of the models for the selected test data, discussions of the effect of the diameters, predictions of the critical flow models, and design aspects of break simulator for SBLOCA scenarios in the IET facilities were presented. In the effect of diameter on the critical flow rate with respect to all dimensional scales, it was concluded that the effect of diameter was found irrespective of diameter sizes. In addition, the diameter effect on slip ratio affecting the critical flow rate was suggested. From a comparison of the critical flow models and selected test data, the Henry-Fauske model of the MARS-KS code was found to be the best model predicting the critical flow rate for the selected test data under study.

Key words : Critical Flow, Discharge Coefficient, Break Simulator, SBLOCA, Sub-cooled/Saturated

1. Introduction

In the safety analysis of loss-of-coolant-accident (LOCA) scenarios of light water reactors, a modeling of a break is very important to predict the accident's result. For example, the design of a break simulator to simulate a SBLOCA in a light water reactor requires an accurate knowledge of the break flow of sub-cooled and saturated water through the break, whose shape can be assumed as an orifice or a nozzle according to its characteristics of the break. In case of the SBLOCA scenario, the critical flow mostly occurs by sub-cooled and saturated water at relatively high pressure conditions. In earlier studies [1-6], most of the information available in the literature was either for a saturated two-phase flow or sub-cooled water flow at medium pressure conditions, e.g., up to about 7.0 MPa. In addition, Chun et al. [7] developed a correlation for predicting the critical flow characteristics for sub-cooled water passing through break simulators of a nozzle type.

The choking is regarded as a condition of maximum possible discharge through a given orifice and/or nozzle exit area. A critical flow rate can be achieved at a choking under the given thermo-hydraulic conditions. The critical flow phenomenon hadbeen studied extensively in both single-phase and two-phase systems because of its

†To whom corresponding should be addressed.
Thermal Hydraulics Safety Research Division, Korea Atomic Energy Research Institute 1045 Daedeokdaero, Yuseong-gu, Daejeon 305-353, Rep. of Korea
Tel : 042-488-3454 E-mail : yskim3@kaeri.re.kr

importance in the LOCA analyses of light water reactors and in the design of other engineering areas. A more detail review for previous analytical and experimental works on critical flow phenomena can be found in reference [8]. Park [8] suggested a modified correlation for predicting the critical flow for sub-cooled water through a nozzle rather than that of Chun et al. [7] which can also be seen in reference [9]. Recently, Park et al. [11] performed an experimental study on a two-phase critical flow with a non-condensable gas under high-pressure conditions. Various experiments of critical flow using a sub-cooled water were performed for a modeling of break simulators in thermo-hydraulic IETfacilities for light water reactors, e.g., advanced power reactor 1400MWe (APR1400) and system-integrated modular advanced reactor (SMART). For the design of break simulators of SBLOCA scenarios, the aspect ratio, L/D, is considered to be a key parameter to determine the shape of the break simulator. Typical shapes of the break simulator could be divided into 2 types of an orifice and a nozzle (or pipe) based on the aspect ratio. An orifice, for example, is in the aspect ratio ofless than 2.5, and a nozzle (or pipe), greater than 2.5.

In this paper, an investigation of the critical flow phenomena was performed especially on break simulators for LOCA scenarios in the IET facilities, e.g., ATLAS [12] and FESTA [13],which simulate the thermal-hydraulic behaviors of APR1400 and SMART, respectively.

2. Review of the Critical Flow Rate Models for Sub-cooled and Saturated Water

As is well known, there have been various studies on the critical flow models for sub-cooled and/or saturated water. In particular, Fauske [1], Moody [3], and Henry [4] suggested basic theoretical models based on their own assumptions, and Zaloudek [2] provided insight into physical phenomena for a critical flow in an orifice type flow path. Sozzi & Sutherland [5] performed a critical flow test of saturated and sub-cooled water at high pressure for orifice and nozzles. In addition, a full-scale critical flow test [6] was also performed under a multi-national project.

In this section, previous studies related to the critical flow rate for sub-cooled and saturated water were reviewed including tests performed at KAERI related to the break simulators in IET facilities [7-11].

2.1 Fauske's Model [1]

Fauske performed a critical flow test of a two-phase separated flow for long tubes, e.g., 3.2 mm (1/8 in.) and 6.8 mm (0.269 in.) in diameter, and 1,428.8 mm (56-1/4 in.) and 2,794.0 mm (110 in.) in length, respectively, whose aspect ratios were 450 and 409, respectively. Although, this study was focused on a saturated two-phase flow, the results were instructive to an understanding of the sub-cooled critical flow.

The definitions used for the author's critical two-phase flow were as follows:

1) The flow is critical when the flow rate no longer increases with increasing pressure difference, i.e., when

$$\left(\frac{dG}{dP}\right)_{constant\ enthalpy} = 0 \quad (1)$$

where, G : mass velocity (kg/m^2-s), and
P : pressure (Pa).

2) Under conditions of a critical flow, the pressure gradient along the pipe proceeding to the exit has an absolute, finite maximum possible value for a given flow rate and quality such as

$$\left|\frac{dP}{dL}\right|_{G,x} \approx \left|\frac{\Delta P}{\Delta L}\right|_{G,x} = \{Max.\}_{Finite} \quad (2)$$

where, L : length (m), and
x : quality.

3) The specific volume for a separated

two-phase flow is given by

$$v = \frac{x^2 v_g}{\alpha_g} + \frac{(1-x)^2 v_f}{1-\alpha_g} \quad (3)$$

where, v : specific volume of separated two-phase flow (m^3/kg), and
α_g : void fraction of gas phase.

Fauske showed that an isentropic flow condition would not be compatible with Eq. (2), and thus a non-isentropic flow where the friction is not zero, was considered, and the slip ratio was obtained as

$$k = (v_g/v_f)^{1/2} = f(P) \text{ for } 0 < x < 1$$
; k=1 for x=0 and x=1 (4)

where, k : slip ratio between gas and liquid phases, defined as $k = u_g/u_f$,
u_g : gas phase velocity (m/s)
u_f : liquid phase velocity (m/s)
v_g : specific volume of gas phase (m^3/kg),
v_f: specific volume of liquid phase (m^3/kg),
P : pressure (Pa), and
x : quality.

A theoretical expression for the critical flow rate from the equation of motion was derived as follows:

$$G_c = \left[\frac{-k}{\{(1-x+kx)x\}\frac{dv_g}{dP}+\{v_g(1+2kx-2x)+v_f(2xk-2k-2xk^2+k^2)\}\frac{dx}{dP}+\{k[1+x(k-2)-x^2(k-1)]\}\frac{dv_f}{dP}}\right]^{1/2} \quad (5)$$

Here, all properties were defined at the throat location where the choking occurs.

In addition to the author's own critical flow rate expression, Eq. (5), Fauske suggested a homogeneous flow model (HFM) for a critical flow rate. The conditions for the HFM were as follows:

1) Adiabatic and reversible expansion;
2) Thermodynamic equilibrium; and
3) Equal phase velocities.

A theoretical critical mass velocity derived from the HFM was given by

$$G_c = \left[\frac{-1}{\left(\frac{dv}{dP}\right)_{sm}}\right]^{1/2} \quad (6)$$

where, v: specific volume (m^3/kg), defined as

$v = v_f(1-x) + v_g x$, and

sm: mean entropy (J/kg-K), defined as

$sm = s_f + s_{fg} x$.

Here, it is noteworthy that all properties for Eqs. (5) and (6) should be defined at the throat location where the choking occurs.

2.2 Zaloudek's Model [2]

Zaloudek performed a critical flow test of hot water through short tubes, e.g., 12.7 mm (0.5 in.) in diameter and 6.4 to 76.2 mm (1/4 to 3 in.) long. He found that there were two kinds of critical flow modes, e.g., the first-step-critical and second-step-critical dependent on the degree of sub-cooling. For avery low temperature, e.g., 20 °C (68°F), there was only one critical mode, i.e., the first-step-critical. The data points falling on the first-step-critical, the pressure near the entrance of the test section remained fixed at a value near the saturation pressure and the entrance region was the choking location. In the second-step-critical, the pressure near the entrance decreased from the saturation value and the location of choking moved to the terminus of the test section.

Test results showed that the mass velocity at which the first-step-critical occurred (G_c) could be correlated by a form of the following formula:

$$G_c = C_1\sqrt{2\rho(P_{up} - P_{sat})} \quad (7)$$

where, C_1: the adiabatic coefficient of discharge, e.g., ~ 0.61-0.64 for the configuration under study,
ρ: density of liquid (kg/m^3),
P_{up}: upstream stagnation pressure (Pa), and
P_{sat}: saturation pressure for upstream temperature (Pa).

For the second-step-critical flow data, the

critical mass velocity (G_c) could be correlated as follows:

$$G_c = \sqrt{2\rho(P_{up} - (1 - C_2)P_{sat})} \quad (8)$$

where, ρ: density of liquid (kg/m^3),

P_{up} : upstream stagnation pressure (Pa), and
P_{sat}: saturation pressure for upstream temperature (Pa).
C_2 : a coefficient defined as $K\frac{\sigma \text{ for saturation pressure}}{\sigma \text{ for 1.3789 MPa (200 psia) saturation pressure}}$
K : an experimentally determined coefficient, e.g., 0.284, and
σ : surface tension (N/m).

In Eq. (8) of the second mode, coefficient C_2includes the effect of surface tension which delays the formation of vapor bubbles. In a practical view point, most of the critical flows occur at the second mode.

2.3 Moody's Model [3]

Moody suggested a theoretical maximum two-phase flow rate using an ideal nozzle and two-phase annular flow properties. Although, this study was focused on the saturated two-phase flow, the result would be instructive to an understanding of the sub-cooled critical flow. Actually, Moody's other study [15] was performed on a maximum two-phase flow rate for a homogeneous, equilibrium two-phase flow including thesub-cooled condition.

An equilibrium maximum two-phase flow rate per unit area, G, was suggested as follows:

$$G = \rho'''[2(h_0 - h(P, s_0)]^{1/2} \quad (9)$$

where, G : maximum two-phase mass flux (kg/m^2-s),
ρ''' : energy density (kg/m^3), defined as $\rho''' = \{[\frac{x}{\rho_g} + \frac{k(1-x)}{\rho_f}][x + \frac{1-x}{k^2}]^{1/2}\}^{-1}$,
$h(P,s_0)$: enthalpy (J/kg), defined as $h(P, s_0) = h_f + \frac{h_{fg}}{s_{fg}}(s_0 - s_f)$, and
s_0 : stagnation entropy (J/kg-K), defined as $s_0 \approx s_f + x s_{fg}$.

As can be seen in Eq. (9), the maximum mass flux, G, is a function of pressure, P, and slip ratio, k. That is, for a knownstagnation state, local static pressure and slip ratio, the critical mass flux can be uniquely determined. If both P and k are considered independent, a maximum G corresponds to the conditions,

$$(\frac{\partial G}{\partial k})_P = 0;\ (\frac{\partial^2 G}{\partial k^2})_P < 0, \quad (10)$$

and

$$(\frac{\partial G}{\partial P})_k = 0;\ (\frac{\partial^2 G}{\partial P^2})_k < 0. \quad (11)$$

For the condition of Eq. (10), it follows from Eq. (9) that at a maximum flow,

$$k = (v_g / v_f)^{1/3}. \quad (12)$$

Eq. (12) shows that at a maximum G, the slip ratio is a function of pressure only. Employing Eq. (12) in Eq. (11) and using saturated steam-water properties, the critical mass flux, G_c, can be obtained in terms of P_0 and h_0.

It is noteworthy that in contrast to Fauske's model [1] which is concerned with local properties at the nozzle throat, Moody's model is concerned only with the upstream stagnation properties. For a blowdown analysis from long pipes, it is necessary to incorporate wall friction effects. In Moody's study [14], the effects of pipe friction on a two-phase maximum flow rate had been suggested. A homogenous equilibrium model(HEM) was also suggested in Moody's other study [15] for both sub-cooled and saturated states.

2.4 Henry's Model [4]

Henry performed a critical flow test of a two-phase separated flow for three test sections, e.g., two circular cross-sections of 8.0 mm (0.313 in.) and one rectangular cross-section, e.g., 23.6 mm × 3.3 mm (0.930 in. × 0.131 in.), of 5.8 mm

(0.230 in.) in diameter and 914.4 mm (36 in.) in length. Although this study was focused on a saturated two-phase flow, the result would be instructive to an understanding of a sub-cooled critical flow.

Most of the assumptions used for the general expressions for a single- and two-phase critical flow were similar to those of Fauske's study [1], and the results can be presented as follows:

$$G_c = \left[\frac{-k}{\{(1-x+kx)x\}\left(\frac{dv_g}{dP}\right)_{h_0} + \{v_g(1+2kx-2x)+v_f(2xk-2k-2xk^2+k^2)\}\left(\frac{dx}{dP}\right)_{h_0} + \{x(1+x(k-2)-x^2(k-1))\}\left(\frac{dv_f}{dP}\right)_{h_0} + x(1-x)\left(kv_f - \frac{v_g}{k}\right)\left(\frac{\partial k}{\partial P}\right)_{h_0}}\right]^{1/2} \quad (13)$$

Here, all the partial derivatives should be defined based on a constant stagnation enthalpy compared to those of Fauske's in Eq. (5),which were defined at the throat location. Like Fauske's model, all properties except partial derivatives for Eq. (13) should be defined at the throat location where the choking occurs.

Henry discussed the reason for an under-prediction of the maximum flow rate by a homogeneous equilibrium model with respect to the experimental data. One is the density difference between the phases that allows a greater acceleration of the gas than the liquid for the same pressure decrease which is greater than unity. The other is the system pressure near the exit plane decreasesso rapidly that the phase change cannot follow an equilibrium process. These two phenomena would decrease the compressibility of the system, and thus results in a flow rate greater than the equilibrium case.

Using the order-of-magnitude approximation, the experimental fact that the velocity ratio, k, is

$$k \sim 0(1) \ll \left(v_g / v_f\right)^{\frac{1}{2}} \sim 0(10), \quad (14)$$

Eq. (13) can be simplified as follows:

$$G_c = \left[\frac{-k}{\{(1-x+kx)x\}\left(\frac{dv_g}{dP}\right)_{h_0} + v_g(1+2kx-2x)\left(\frac{dx}{dP}\right)_{h_0} - x(1-x)\frac{v_g}{k}\left(\frac{\partial k}{\partial P}\right)_{h_0}}\right]^{1/2} \quad (15)$$

Henry discussed the slip between phases, and the effects of retarded phase change are interdependent which can be presented as follows:

$$k = \frac{x}{1-x}\frac{1-\alpha}{\alpha}\frac{v_g}{v_f} \quad (16)$$

where, is a void fraction. When the specific volumeratio and void fraction are determined experimentally, the actual slip or velocity ratio, k, can only be calculated using Eq. (16) if the real quality is known. Henry mentioned that the exit velocity ratio of the reference point (k_{Ee}=1.3) was the maximum exit velocity ratio in the range investigated, then the exit velocity ratios would always be near unity for low-quality flows, e.g., actual velocity ratio between 1.0 and 1.3.

It is noteworthy that Henry discussed a frozen model, in which there was no phase change, and thus $(x/P)_{h0}$ = 0. This concept would be applicable to a two-component flow, e.g., air-water flow.

2.5 Sozzi & Sutherland's Test [5]

Sozzi and Sutherland performed critical flow rateexperiments for sub-cooled and saturated water to determine the effect of fluid enthalpy, flow geometry and size, and flow length. Tests were conducted by blowing down vessels from an initial fluid pressure of 6.895 MPa with the discharge fluid temperature between 232 and 288 °C. The results clearly demonstrate the influence of metastable,and/or non-equilibrium, thermodynamic states for flow lengths of less than about 127 mm. Data for different diameter nozzles, from 12.7 to 76.2 mm, showed that the critical mass flux decreased with an increase in diameter.

2.6 Marviken test [6]

The Marviken full-scale critical flow tests (CFT) were conducted between mid-1977 and December 1979 as a multi-national project at the Marviken

Power Station. A total of 27 CFTs were conducted by discharging water and steam-water mixtures from a full sized reactor vessel through a large diameter discharge pipe that supplied the flow to the test nozzle. The nine test nozzle geometries all had rounded entrances followed by a nominally 200, 300 or 500 mm constant diameter cross-section. The nozzles ranged in length from 166 to 1809 mm.

Most tests were conducted with a nominal initial steam dome pressure of 5 MPa (4 MPa for one test) and with the water initially sub-cooled between 50℃ and 1℃ (with respect to the steam dome pressure). The water oxygen content was approximately the same for all tests, but it was decreased by a factor of 140 with respect to a reference test in order to determine the effect of the air-water content on the critical mass flow rate.

The vessel, discharge pipe,and nozzle were instrumentedto determine the test behavior and provide a basis for evaluating the stagnation conditions and mass fluxes at the nozzle inlet. The instrumentation readings were recorded using a pulse code modulation system. Data error limits were evaluated for all measurements.

2.7 Tests for IET Facilities in KAERI [7-11]

Park [8], including studies of Chun et al. [7] and Park et al. [9], performed critical flow rate tests of sub-cooled water through short pipes (L 400 mm) with small diameters (D 7.15 mm) for wide ranges of sub-cooling (0-199 ^{o}C) and pressure (0.5-2.0 MPa). These tests were focused on the effects of various parameters, e.g., the location of flashing inception, the degree of sub-cooling, the stagnation temperature and pressure, and the pipe size related to the critical flow rates of sub-cooled water through short pipes with small diameters, and a total of 135 runs were made for various combinations of the test parameters using four different L/D test sections. (All data of the 135 runs could be referred to Park's thesis [8].)

Using the test data, an empirical correlationof the critical flow rate for sub-cooled water was developed as follows:

$$G_c = (C_d)_{ref}[2\rho_{ref}(P_0 - P_b)]^{1/2}\{1 - \frac{15.2}{1+e^{[(\Delta T^*_{sub}+0.578)/0.188]}}\} \quad (17)$$

where, $(C_d)_{ref}$: reference discharge coefficient, defined as $(C_d)_{ref} = (1 + K + f\frac{L}{D})^{-1/2}_{ref}$,
K : form loss coefficient,
f : fanning friction factor,
L : length (m),
D : inner diameter (m),
ρ_{ref}: density at reference condition (kg/m^3),
P_0 : stagnation pressure (Pa),
P_b : back pressure (Pa), and
ΔT^*_{sub} : dimensionless sub-cooling, defined as $\Delta T^*_{sub} = \frac{T_{sat}-T_0}{T_{sat}-T_{ref.}}$

Here, subscript '*ref*' represents properties defined at 20 ^{o}C under atmospheric conditions.

As can be seen in Eq. (17), Park [8] adopted the back pressure as a reference pressure for the critical flow rate prediction and concluded that a good agreement was confirmed from comparisons between the mass fluxes using the correlationand a total of 755 selected experimental data points of nine different investigators. In most of the previous studies, the back pressure was not found as a reference pressure for the critical flow phenomena. Therefore, it is recommended that discretion should be considered for the use of Eq. (17).

Park el al. [10] also performed another test for critical flow rates through square edge orifices to evaluate the performance of a break simulator design for small break accidents in IET facilities. Steady state and blowdown critical flow tests had been performed using eight different square shape edge orifices. The steady state flow data show that the maximum mass flux can be expressed as a function of discharge coefficient and stagnation condition. Based upon the test results, another empirical correlation had been developed using the form of a previously developed one, i.e., Eq. (17), as follows:

$$G_c = (C_d)_{ref}[2\rho_{ref}(P_0 - P_b)]^{1/2}\{1.04 - \frac{3.28}{1+e^{[(\Delta T^*_{sub}+1.1)/0.488]}}\} \quad (18)$$

Park et al. [11] performed an experimental study on a two-phase critical flow with non-condensable gas under high-pressure conditions. Experimental data for the critical flow rates were generated using sharp-edged stainless steel pipes with an inner diameter of 10.9 mm and a length of 1,000 mm. The test conditions were varied using stagnation pressures of 4.0, 7.0, and 10.0 MPa, water sub-coolings of 0.0, 20.0, and 50.0℃,and nitrogen gas flow rates of 0.0 to 0.22 kg/s. A comparison between test data without non-condensable gas and predictions of Eq. (17) showed quite a good agreement between them. The experimental results showedthat the critical mass flux decreases rapidly with an increase of the volumetric non-condensable gas fraction. In addition, the critical mass flux increased with an increase in the stagnation pressure and a decrease in the stagnation temperature. An empirical correlation of the non-dimensional critical mass flux which is expressed as an exponential function of the non-condensable gas fraction of the volumetric flow, was obtained from the experimental data as follows:

$$G_c = G_{c0}\left(0.378 + 0.600e^{-(Q_a/Q_{c0})/0.195}\right) \quad (19)$$

where, G_{c0}: reference mass flux without non-condensable gas (kg/m^2-s),
Q_a: volumetric flow rate of the non-condensable gas (m^3/s), and
Q_{c0}: reference volumetric flow rate without a non-condensable gas (m^3/s).

2.8 A Hybrid Concept Considered by the Authors

In the above sections, typical models for a critical flow rate for sub-cooled and saturated water were reviewed. The authors found that each model had its own characteristics and some attention should be needed for its application. As commented before, Moody's model [3] provides an analytical prediction using upstream stagnation conditions and a steam table. The result includes thecritical flow rate for the given upstream stagnation conditions and local pressure/quality at the choked location. Fauske's model[1] is focused on the local conditions at the choked location, and thus local properties, e.g., pressure and quality, are needed for evaluation. In Fauske's model, upstream stagnation conditions are not considered in its prediction. Henry [4] developed a modified form of Fauske's model including upstream stagnation conditions. As Fauske's model, Henry's model [4] also needs local properties, e.g., pressure and quality even including the slip ratio, for a critical flow rate evaluation. In a practical sense, local properties could be checkedonly by experiment, and thus the application of Fauske and Henry would be very restrictive.

It was well known that Moody's model gives an over-estimation of the critical flow rate rather than the experimental data and Fauske's model [14]. Considering these circumstances, the authors would like to consider a hybrid concept in this paper using Moody's and Fauske's models. The hybrid concept adopts Moody's model for the prediction of local properties under the given upstream stagnation conditions, and Fauske's model for the prediction of critical flow rate using the local properties from Moody's model, respectively.

It is noteworthy that the hybrid concept had a limitation for the prediction of the critical flow rate owing using of Moody and FauskeModels. In their models, slip ratios defined by different physical senses were adopted, respectively. The slip ratio in the Moody Model tended to induce an over-estimation of the critical flow rate. In this respect, the hybrid concept tends to over-estimate the critical flow rate.

3. Comparison of Critical Flow Rate Models for Selected Test Data

It is an instructive work to compare the critical flow ratetest data and predictions by models reviewed in the previous section. In this section, the

Table 1. Comparison of selected test data from Fauske [1]

D(mm)	L/D	Upstream(P_6[a];MPa)	G_c(kg/m^2-s)	Remark[b]
6.83	408.9	1.76	5,607.6	TSII-5
3.18	450.0		8,306.1	TSIV-3
6.83	408.9	2.65	5,016.8	TSII-64
3.18	450.0		6,912.7	TSIV-4
6.83	408.9	2.72	4,766.0	TSII-65
3.18	450.0		13,825.3	TSIV-7

Note. a: P_6 in the report was selected for the upstream pressure.
b: Run number defined in the report.

Table 2. Comparison of selected test data from Park [8]

D(mm)	L/D	P_0(MPa)[a]	T_0(^{o}C)[a]	$\triangle T_{sub}$(^{o}C)	G_c(kg/m^2-s)	Remark[b]
7.1	28.2	1.0	178.5	1.3	9,782	81
3.4	29.4		179.9	0.0	9,847	11
7.1	28.2	1.5	196.1	2.0	11,050	93
3.4	29.4		198.0	0.1	12,042	22
7.1	28.2	2.0	191.1	20.3	23,921	107
3.4	29.4		191.9	20.1	30,583	36

Note. a: Upstream stagnation conditions for sub-cooled water
b: Run number defined in the report.

selected test data related to sub-cooled and saturated water were used for discussions of the effect of the diameters, predictions of the critical flow models, and design aspects of break simulators for an SBLOCA in IET facilities.

3.1 Discussions on the Effect of Diameters

The critical flow rate was originated to investigate the safety analysis of real nuclear power plants. These safety analyses assumed a kind of spectrum of pipe breaks in the nuclear steam supply system of a nuclear power plant. Many studies were performed on the development of theoretical and/or empirical models to predict the real critical flow phenomenon. Owing to the limitation of scale, most of the experiments were performed for relatively small sizes, especially in diameter.

As described before, Sozzi and Sutherland [5] found that the critical mass flux decreases with an increasing diameterbased on data for four different diameter nozzles, from 12.7 to 76.2 mm. Data for nozzles 3 and 5-7 in the appendix of their report [5] showed such trends. Actually, nozzle 3 was a sharp-edged orifice with an aspect ratio of 0.37.

The diameter effect was also found in quite a long pipe. Fauske [1] performed saturated two-phase critical flow tests using fairly long pipes with small diameters, whose aspect ratios are 408.9 and 450.0, respectively. As shown in Table 1, the measured saturated two-phase critical flow rates increased with decreasing diameter. In a smaller diameter, e.g., 3.18 mm, the aspect ratio was greater than that of a larger diameter, e.g., 6.83 mm, and the measured flow rates of a smaller diameter were larger than those of a larger one. Actually, the critical flow rate can be affected by the friction effect, e.g., a larger friction and smaller critical flow rate, as commented by Moody [15]. Although the friction was larger in the case of a smaller diameter, the measured critical flow rate was larger, which means that the diameter effect can be dominant for the critical flow rate within the configuration under study.

The diameter effect was also found in a relatively short pipe, whose aspect ratio is about 30. Park [8] performed a critical flow test with sub-cooled water at the nozzle entrance using medium lengths with small diameters, whose L/D

Table 3. Comparison of selected test data from Marviken [6]

D(mm)	L/D	Inlet P(MPa)[a]	Inlet T(°C)[a]	△ T_{sub}(°C)	G_e(kg/m^2-s)	Remark[b]
509	3.1	4.32	237_{sub}[c]	16.0	45,522.5	4
300	3.0		242_{sub}	11.0	41,691.5	2
509	3.1	4.09	251_{sat}[d]	0.0	19,141.8	4
300	3.0		251_{sat}	0.0	29,779.7	2
509	3.1	3.87	247_{sat}	0.0	17,072.8	4
300	3.0		247_{sat}	0.0	21,588.5	2

Note a: Properties at inlet ring 1.
b: Figures are the test numbers defined in the report.
c: Mean temperature; subscript 'sub' means sub-cooled water.
d: Subscript 'sat' means saturated water.

are 28.2and 29.4, respectively. The measured sub-cooled water critical flow rates increased with a decreasing diameter, as shown in Table 2.

Park et al. [10] found that measured critical flow rates using sharp edge orifices for sub-cooled water also showed similar diameter effects. However, in their paper, it was concluded that the effect of orifice diameter for the same L/D geometry could not beidentified due to the contradiction between the theoretical and measured aspects.

In general, friction and/or form loss are considered to affect the critical flow rate. Moody [15] suggested a theoretical study including the friction effect on the critical flow rate. From the viewpoint of form loss, smaller diameters in the pipe or nozzle/orifice induce larger form-loss coefficients, indicating that the expected critical flow rates through the pipe or nozzle/orifice with smaller diameters would be smaller values than those of larger diameters. In a real case, however, most of the test data with different diameters which were used to identify the diameter effect on the critical flow rates for sub-cooled and saturated two-phase water, showed that the measured sub-cooled and saturated two-phase critical flow rates increased with decreasing diameters. This seemed to give a kind of contradiction between the theoretical and measured situations to the authors. After a review of the theoretical models for critical flow rate, e.g., Fauske's and investigators' models, the authors assumed here that the physical reason of the diameter effect on the critical flow rate is mainly due to the slip ratio at choked location. If a slip occurs in a flow path like a pipe or nozzle/orifice, the slip effect can be relatively emphasized for smaller diameters rather than larger ones [16].

To check the effect of diameter with respect to the wider ranges of dimension, the authors investigated the real plant-scale data from a Marvikentest [6]. Fortunately, proper data with the same ratio of L/D were available for comparison. Although the gained data show some errors from reading the data from the figures, the overall trend could be identified qualitatively, as shown in Table 3. In Table 3, a comparison of the measured critical flow rates for sub-cooled water would be meaningless related to the diameter effect, because the critical flow rates are very sensitive to the degree of sub-cooling, e.g., a larger sub-cooling and larger critical flow rate. Thus, in this sub-cooling case, there was no basis for the diameter effect on the critical flow rates. However, the measured critical flow rates for saturated water showed similar effects of diameter on the measured critical flow rates, as shown in Table 3. From these considerations, there must also be a diameter effect on the critical flow rates in a real scale.

From the review of the effect of diameter on the critical flow rate with respect to all the dimensional scales, it was concluded that the effect of diameter was found irrespective of diameter sizes. Although

Table 4. Selected test data for comparison of critical flow rate models

No.	D(mm)	L(mm)	L/D	Inlet P(MPa)	Inlet T(°C)	G_c(kg/m^2-s)	Uncertainty[e](%)	Condition[d]	Remark
1[a]	12.7	4.7	0.37	6.412	241.7	59,029.5	NA[f]	sub-cooled	Orifice
2[a]	12.7	4.7	0.37	6.412	266.1	53,795.5		sub-cooled	Orifice
3[a]	12.7	4.7	0.37	6.378	279.6	52,267.3		saturated	Orifice
4[b]	3.4	100	29.4	1.001	179.9	9,847.0	NA[f]	sub-cooled	Pipe
5[b]	3.4	100	29.4	1.495	198.0	12,042.0		sub-cooled	Pipe
6[b]	3.4	100	29.4	1.985	191.9	30,583.0		sub-cooled	Pipe
7[b]	7.1	200	28.2	0.999	178.5	9,782.0		sub-cooled	Pipe
8[b]	7.1	200	28.2	1.495	196.1	11,050.0		sub-cooled	Pipe
9[b]	7.1	200	28.2	1.961	191.1	23,921.0		sub-cooled	Pipe
10[c]	300	895	3.0	4.315	242.0	41,691.5	Sub-cooled:±10; Two-phase:±15	sub-cooled	Pipe
11[c]	300	895	3.0	3.873	247.0	21,588.5		saturated	Pipe
12[c]	300	895	3.0	4.085	251.0	29,779.7		saturated	Pipe
13[c]	509	1,589	3.1	4.315	237.0	45,522.5		sub-cooled	Pipe
14[c]	509	1,589	3.1	3.873	247.0	17,072.8		saturated	Pipe
15[c]	509	1,589	3.1	4.085	251.0	19,141.8		saturated	Pipe

Note a: Data from Sozzi &Sutherland [5].
b,c: Data from Tables 2 and 3, respectively.
d: Liquid (or water) flow for sub-cooled and saturated conditions.
e: Uncertainty of measured critical mass flux.
f: NA means 'not available'.

interim stage, it was suggested that a possible parameter affected by the effect of diameter be a slip ratio between phases. Henry [4] discussed the effect of slip ratio on his theoretical model and concluded that the slip ratio was within a limited range of 1.0-1.3 which should be identified experimentally. In this paper, the authors would like to suggest the diameter effect on slip ratio deliberately and reserve it as a further work of this study.

3.2 Comparisons of Critical Flow Rate Models Using Selected Test Data

It would be very instructive to compare the critical flow models discussed in the previous sections and the selected test data for an evaluation of themodels. For the selected test data, the data in Tables 2 and 3 including selected data from Sozzi and Sutherland [5], as shown in Table 4, are used. All data in Table 4 were critical flow tests for sub-cooled water or saturated water. The data in Table 1 were only for a saturated two-phase water flow, whose inlet properties, e.g., void fraction and/or quality, could not be defined in report [1]. For this reason,the data of Table 1 were excluded in Table 4.

In addition, it would be productive to compare the critical flow rates calculated using safety analysis codes, e.g., MARS-KS [17] and TRACE [18]. In the MARS code, there are two types of critical flow rate models, e.g., Henry-Fauske and Trapp-Ransom models. For the simplification, default options were used in this study, which are summarized for MARS-KS calculations as follows:

1) Henry-Fauske critical flow ($MARS_{H-F}$)
   - Discharge coefficient : 1.0
   - Thermal non-equilibrium constant : 0.14, and

2) Trapp-Ransom critical flow ($MARS_{T-R}$)
   - Sub-cooled discharge coefficient : 1.0
   - Two-phase discharge coefficient : 1.0
   - Superheated discharge coefficient : 1.0.

Like the case of MARS-KS, the default options of the critical flow rate were used in the calculation of TRACE, too.

A summary of the calculation results is shown in Table 5. For Zaloudek's calculation, the correlationof critical mass velocity for the second-step-critical flow, e.g., Eq. (8), was used. As shown in the table, a large amount of over-prediction was found. For Moody's calculation, Eqs. (9)-(11) could be used for the saturated

Table 5. Summary of the calculation results (unit: kg/m2-s)

No.	Test Data	Zaloudek[2]	Moody[3] [a]	Hybrid[a]	Park[9,10][b]	$MARS_{H-F}$[17][c]	$MARS_{T-R}$[17][c]	TRACE[18] [c]	Remark
1	59,029.5	77,277.3	NA	NA	59,377.0	61,993.2	58,856.8	56,739.5	Orifice; Sub-cooled
2	53,795.5	56,754.2	NA	NA	55,992.6	55,547.6	55,618.7	72,497.2	Orifice; Sub-cooled
3	52,267.3	36,509.2	37,151.9	35,535.2	53,670.9	45,924.7	36,438.4	71,069.1	Orifice; Saturated
4	9,847.0	23,393.8	NA	NA	9,927.3	8,416.8	5,533.2	7,172.7	Pipe; Sub-cooled
5	12,042.0	26,942.3	NA	NA	12,430.7	11,599.0	7,874.7	9,367.1	Pipe; Sub-cooled
6	30,583.0	42,926.6	NA	NA	26,526.1	25,711.5	24,356.8	22,134.1	Pipe; Sub-cooled
7	9,782.0	24,242.8	NA	NA	11,460.3	9,001.6	7,154.7	7,467.7	Pipe; Sub-cooled
8	11,050.0	28,451.6	NA	NA	14,675.2	12,586.2	10,102.6	9,986.1	Pipe; Sub-cooled
9	23,921.0	42,821.5	NA	NA	28,237.6	26,480.1	25,586.0	23,130.5	Pipe; Sub-cooled
10	41,691.5	50,227.6	NA	NA	43,801.0	44,562.0	42,701.6	32,441.4	Pipe; Sub-cooled
11	21,588.5	36,548.0	29,311.6	27,552.7	27,624.2	26,532.9	19,470.7	20,145.6	Pipe; Saturated
12	29,779.7	35,767.1	30,074.6	28,343.5	28,389.9	26,250.0	20,294.0	20,838.8	Pipe; Saturated
13	45,522.5	54,507.5	NA	NA	48,480.7	47,962.5	47,256.3	37,501.1	Pipe; Sub-cooled
14	17,072.8	36,548.0	29,311.6	27,552.7	27,624.2	23,150.5	16,848.2	20,417.8	Pipe; Saturated
15	19,141.8	35,767.1	30,074.6	28,343.5	28,389.9	22,708.2	19,260.2	21,056.9	Pipe; Saturated

Note a: NA means that authors could not obtain calculation results using an in-house steam table.
b: Underlined data were obtained for saturated condition.
c: Underlined data mean flow rates with no occurrence of choking at the test section itself.

Table 6. Summary of R2-values for each model with respect to test data

Zaloudek	Moody	Hybrid	Park	$MARS_{H-F}$	$MARS_{T-R}$	TRACE
0.730	0.915	0.915	0.951	0.957	0.924	0.857

condition. For a sub-cooled condition, Moody's other method [19] could be used. It was found that the HEM method could be used for a small sub-cooled condition, e.g., sub-cooling less than 5 ^{o}C. However, for a larger sub-cooled condition, e.g., sub-cooling greater than 5 ^{o}C, it was very hard to obtain a suitable result using the HEM method. For this reason, most of the sub-cooled data were unavailable for Moody's calculation in the table. As considered by the authors, the calculation results using a hybrid concept which uses Moody's and Fauske's models at the same time, are shown in the table. For sub-cooled conditions, Moody's data were not available in this study, and thus there were no data for a hybrid model, either. For Park's calculation, different equations were used for orifice and pipe flows, e.g., Eq. (17) for a pipe flow and Eq. (18) for an orifice flow. For information, all the reference discharge coefficients used for Eqs. (17) and (18) could be referred to Appendix 'A' of this paper. Although, Eqs. (17) and (18) adopted the back pressure as a reference pressure, the calculation results showed quite a good trend. For MARS' calculation, the default options were used for Henry-Fauske and Trapp-Ransom models. As shown in the table, Henry-Fauske model showed very good predictions with respect to the test data. In general, the Trapp-Ransom model under-predicted that of the Henry-Fauskemodel. For TRACE's calculation, the default options of critical flow rate were used in the calculation, and the calculation results showed a relatively good trend with respect to the test data. For a quantitative comparison, the degrees of correlation between the model's prediction and test data, e.g., a coefficient of determination (R^2-value), were evaluated for each model, as shown in Table 6. As shown in the table, the best model for a critical flow rate prediction was Henry-Fauske model of the MARS code for selected test data under study followed by Park's model.

It is noteworthy that in the test of a critical flow rate, the test facility should be designed cautiously to avoid choking outside of the test

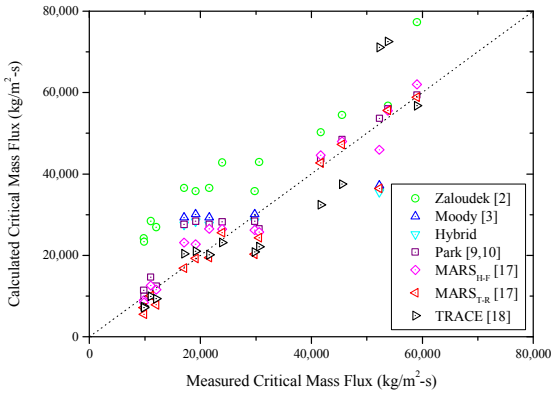

Fig. 1. Comparison between model calculations and selected test data

section itself, especially downstream of the test section. For most of the calculation data underlined in Table 5 for MARS and TRACE calculations, the choking locations were found downstream of the test section. This means that the measured data could be the critical flow rates for the test facility, and not for the test section.

For a qualitative comparison, all data were displayed in a figure, as shown in Fig. 1.

3.3 Discussions on Design Aspects of Break Simulators for SBLOCA in IET Facilities

Break simulators for SBLOCA scenarios in the IET facilities of KAERI, e.g., ATLAS and FESTA, were designed by Park's model [9]. The shapes of the break simulators were a bell-mouthed or sharp-edged pipe (or nozzle) type with respect to the required total loss coefficient. In the SBLOCA scenarios of ATLAS, the sequence of events typically consisted of a blowdown, pressure plateau, loop seal clearing, boil-off, and core recovery. From the blowdown to loop seal clearing phases, the break flow was sub-cooled and/or saturated water. After the loop seal clearing phase, the break flow changed into a steam-water two-phase flow. However, in the SBLOCA scenarios of FESTA, the break flow was sub-cooled and/or saturated water for all the sequence of events of the SBLOCA scenarios. In this circumstance, the designed break simulators are able to introduce some distortion of the break flow rate for the later phases of the SBLOCA scenarios in ATLAS. As discussed before, Park's correlation, i.e., Eq. (17), was developed for sub-cooled and/or saturated water conditions. In the later phases of the SBLOCA scenarios in ATLAS, the break flow changed into a two-phase steam-water condition. Thus, itis instructive to review the effect of break simulator in ATLAS for a two-phase steam-water break flow. To evaluate Park's model for two-phase steam water condition, data of Table 1 were selected as the reference data for the comparison of two-phase steam-water critical flow rates. A summary of the comparison for the selected data is shown in Table 7. As can be seen in the table, Park's model showed quite a large deviation compared to the test data, in general. This means that the design of a break simulator based on Park's model in ATLAS should be cautious on the effect of a two-phase steam-water break flow in the later phases of the SBLOCA scenario. The R^2-value was evaluated as 9.47E-4 which means that Park's model is little correlated with two-phase steam-water critical flow test data. Actually, Park's model did not consider the stagnation enthalpy as a reference enthalpy, and it could hardly calculate the critical flow rate under a

Table 7. Comparison of two-phase critical flow for selected data

No.	D(mm)	L(mm)	L/D	Inlet P(MPa)	Inlet T(°C)	h_c(kJ/kg)	G_c(kg/m²-s)	Park, Eq.(17)
1	3.18	1431	450	1.76	206.0	996.8	8,306.1	6,040.8
2	3.18	1431	450	2.65	227.1	1,167.1	6,912.7	7,488.1
3	3.18	1431	450	2.72	228.5	947.0	13,825.3	7,590.2
4	6.83	2793	408.9	1.76	206.0	1,162.9	5,607.6	6,302.1
5	6.83	2793	408.9	2.65	227.1	1,638.4	5,016.8	7,812.0
6	6.83	2793	408.9	2.72	228.5	1,814.9	4,766.0	7,918.5

two-phase steam-water flow as a stagnation condition.

In Table 7, the authors added estimated enthalpies at choked location, e.g., h_c, for information as enthalpies for stagnation conditions were unavailable in the reference.

4. Summary and Conclusions

In this study, various studies on the critical flow models for sub-cooled and/or saturated water were reviewed, especially on Fauske, Moody, and Henry for basic theoretical models Zaloudek for the insight of physical phenomena for critical flow in an orifice type flow path Sozzi and Sutherland for a critical flow test of saturated and sub-cooled water at high pressure for orifice and nozzles; and a Marviken test on a full scale critical flow test. In addition, critical flow tests of sub-cooled water for the break simulators in IET facilities werealso investigated, and a hybrid concept using Moody's and Fauske's models was considered by the authors which adopted Moody's model for the prediction of local properties under the given upstream stagnation conditions and Fauske's model for the prediction of critical flow rate using local properties obtained from Moody's model.

In the comparison among models for selected test data, discussions of the effect of the diameters, predictions of the critical flow models, and design aspects of break simulator for SBLOCA scenarios in the IET facilities were presented. In the effect of diameter on the critical flow rate with respect to all dimensional scales, it was concluded that the effect of diameter was found irrespective of diameter sizes. In addition, thediameter effect on slip ratio affecting the critical flow rate was suggested, which should be investigated as a further work of this study. From a comparison of the critical flow models and selected test data, the Henry-Fauske model of the MARS code was found to be the best model predicting the critical flow rate for the selected test data under study followed by Park's model. This means that Henry-Fauske model is the best candidate critical flow models. From discussions on break simulators for SBLOCA in the IET facilities, Park's model should be used cautiously, especially on a two-phase steam-water flow as a stagnation condition in the later phases of the SBLOCA scenario.

Acknowledgement

This research was supported by the National Research Foundation of Korea (NRF) grant funded by the Korea government (MSIP).

Nomenclature

APR1400	Advanced Power Reactor 1400 MWe
ATLAS	Advanced Thermal-hydraulic test Loop for Accident Simulation
CFT	Critical Flow Test
FESTA	Facility for Experimental Simulation of Transients and Accidents
HEM	Homogeneous Equilibrium Model
HFM	Homogeneous Flow Model
IET	Integral Effect Test
KAERI	Korea Atomic Energy Research Institute
KINS	Korea Institute of Nuclear Safety
LOCA	Loss-of-coolant-accident
MARS-KS	Multi-dimensional Analysis of Reactor Safety - KINS
SBLOCA	Small break loss-of-coolant-accident
SMART	System-integrated Modular Advanced ReacTor

Symbols

A_0 Cross-sectional area (m^2) at throat of test section

A_1 Cross-sectional area (m^2) at inlet of test section

A_2 Cross-sectional area (m^2) at outlet of test section

C_1 Adiabatic coefficient of discharge

C_2 Coefficient, as defined $C_2 = K \frac{\sigma \text{ for saturation pressure}}{\sigma \text{ for 1.3789 MPa (200 psia) saturation pressure}}$

C_d Discharge coefficient

D Throat diameter (m)

f Fanning friction factor

G Mass velocity or flux (kg/m^2-s)

G_{c0} Reference mass flux without non-condensable

gas (kg/m^2-s)
h Enthalpy (J/kg)
k Slip ratio between gas and liquid phases, as defined $k = u_g/u_f$
k_{Ee} Exit velocity ratio of the reference point
K Form loss coefficient or experimentally determined coefficient, 0.284, used in C_2
L Length (m)
P Pressure (Pa)
Q_a Volumetric flow rate of the non-condensable gas (m^3/s)
Q_{c0} Reference volumetric flow rate without a non-condensable gas (m^3/s)
R Radius of curvature (m)
s Entropy (J/kg-K)
R^2 Coefficient of determination obtained by RSQ function
Re Reynolds number, $Re = \rho uD/\mu$
s_0 Stagnation entropy (J/kg-K)
sm Mean entropy (J/kg-K), $sm = s_f + s_{fg}x$
ΔT Temperature difference (°C)
ΔT^*_{sub} Dimensionless sub-cooling, defined as $\Delta T^*_{sub} = \frac{T_{sat}-T_0}{T_{sat}-T_{ref}}$
u Velocity (m/s)
x Quality

Greeks

α Void fraction
φ Parameter, as defined $\varphi(\iota) = 0.25 + 0.535 * \iota^8/(0.05 + \iota^8)$
Parameter, as defined $\iota = L/D$
μ Viscosity (kg/m-s)
ρ Density (kg/m^3)
ρ''' Energy density (kg/m^3)
σ Surface tension (N/m)
τ Parameter, as defined $\tau(\varphi, \iota) = (2.4 - \iota) * 10^{-\varphi}$
v Specific volume (m^3/kg)
ξ Total loss coefficient
ξ' Parameter, as defined $\xi' = 0.03 + 0.47 * 10^{(-7.7*R/D)}$

Superscripts

* Dimensionless quantity

Subscripts

0 Stagnation condition
c Critical or choked condition
fg Difference between saturated vapor and liquid properties
f Liquid or water
g Gas or steam
H-F Henry-Fauske model
ref Reference condition, i.e., properties defined at 20℃ under atmospheric condition
sat Saturated condition
sub Sub-cooled condition
T-R Trapp-Ransom model
up Upstream stagnation condition

References

1. H.K. Fauske: "Contribution to the Theory of Two-phase, One Component Critical Flow," ANL-6633 (1962)
2. F.R. Zaloudek: "Critical Flow of Hot Water through Short Tubes," General Electric, HW-77594 (1963)
3. F.J. Moody: "Maximum Flow Rate of a Single Component, Two-Phase Mixture." ASME Journal of Heat Transfer, pp. 134-142 (1965)
4. R.E. Henry: "A Study of One- and Two-Component, Two-Phase Critical Flows at Low Qualities," ANL-7430 (1968)
5. G.L. Sozzi and W.A. Sutherland: "Critical Flow of Saturated and Subcooled Water at High Pressure," NEDO-13418 (1975)
6. U.S. NRC: "The Marviken Full-Scale Critical-Flow Tests,"NUREG/CR-2671, MXC-301 (1982)
7. M-H. Chun, C-K. Park, and J-W. Park, "An Experimental Investigation of Critical Flow Rates of Subcooled Water Through Short Pipes with Small Diameters," Int. Comm. in Heat and Mass Transfer, Vol. 23, No. 8, pp. 1053-1064 (1996)
8. C-K. Park, "An Experimental Investigation of Critical Flow Rates of Subcooled Water through Short Pipes with Small Diameters,"

Ph. D. Thesis, KAIST, Korea (1997)
9. C-K. Park, J-W. Park, M-K. Chung, and M-H. Chun: "An Empirical Correlation for Critical Flow Rates of Subcooled Water through Short Pipes with Small Diameters," Nuc. Eng. and Tech., Vol. 29, No. 1, pp. 35-44 (1997)
10. C-K. Park, S. Cho, T-S. Kwon, S-K. Yang, and M-K. Chung: "An Experimental Investigation of Maximum Flow Rates of Subcooled Water through Square Edge Orifices with Small Diameters," NTHAS2: Second Japan-Korea Symposium on Nuclear Thermal Hydraulics and Safety, Fukuoka, Japan, Oct. 15-18 (2000)
11. H-S. Park, N-H. Choi, S-K. Chang, C-H. Chung, S-J. Yi, C-K. Park, and M-K. Chung: "Experimental Study on a Two-phase Critical Flow with a Non-Condensable Gas at High Pressure Conditions," Int. J. Multiphase Flow, 33, pp. 1222-1236 (2007)
12. W-P. Baek, and Y-S. Kim, "Accident Simulation ATLAS for APWRs," Nuclear Engineering International, 53, pp. 21-25 (2008)
13. H-S. Park, S-J. Yi, and C-H. Song," SMR Accident Simulation in Experimental Test Loop," Nuclear Engineering International, November, pp. 12-15 (2013)
14. R.T. Lahey, Jr. and F.J. Moody, The Thermal-Hydraulics of a Boiling Water Reactor, 3rd Printing, American Nuclear Society (1984)
15. F.J. Moody, "Maximum Two-Phase Vessel Blowdown from Pipes," ASME Journal of Heat Transfer, pp. 285-295 (1966)
16. S-T. Lee, "Horizontal Disperse Flows: Disperse and Continuous Phase Velocity,"Interim Presentation, Korea Atomic Energy Research Institute (2013)
17. B-D. Chung et al., "MARS Code Manual, Volume II: Input Requirements," KAERI/TR-2811/2004, Korea Atomic Energy Research Institute (2007)
18. U.S. NRC, "TRACE V5.0 User's Manual, Volume 1: Input Specification," Office of Nuclear Regulatory Research, U.S. NRC (2008)
19. F.J. Moody, "Maximum Discharge Rate of Liquid-Vapor Mixtures from Vessels, Non-Equilibrium Two-Phase Flows," ASME Symp.,American Society of Mechanical Engineers, pp. 27-36 (1975)
20. I.E. Idelchik, Handbook of Hydraulic Resistance, 3rd Edition, Begell House, Inc. (1996)

Appendix A. Reference Discharge Coefficient for EQs. (17) and (18)

The reference discharge coefficient, $(C_d)_{ref}$, used in Eqs. (17) and (18) was redefined in this section. To define the reference discharge coefficient, a general pressure drop relation is necessary to be introduced as follows [20]:

$$\Delta P = \zeta \frac{\rho u^2}{2} \tag{A-1}$$

where, P: pressure drop (Pa),
ξ : total loss coefficient,
ρ : density (kg/m^3), and
u: velocity at the throat or smallest cross-section (m/s).

From the comparison of Eq. (17) with Eq. (A-1), the relation between the reference discharge coefficient and total loss coefficient can be defined as follows:

$$(C_d)_{ref} = \zeta^{-0.5} \tag{A-2}$$

In general, the total loss coefficient, , consists of local form loss and friction loss coefficients. The friction loss coefficient is well known as $f \cdot L/D$, here, f is fanning friction factor; L: length (m); D: throat diameter (m). The fanning friction factor is known mainly dependent on the Reynolds number, Re, as follows:

$4000 < Re < 10^5$: $f = 0.3164 / Re^{0.25}$ (A-3)

$10^5 Re$: $f = 1/(1.8 * \log_{10} Re - 1.64)^2$ (A-4)

where, Re: Reynolds number, defined as,

$Re = \rho u D / \mu$

ρ : density (kg/m^3),

u: velocity at the throat or smallest cross-section (m/s),

D: throat diameter (m), and

μ: Viscosity (kg/m-s).

All the total loss coefficients for orifice and pipe in this section were introduced from Idelchik [20] and summarized as follows:

A-1: Thin Sharp-Edged Orifice (L/D<0.015 refer to Fig. A-1)

$$\zeta = [0.707 * (1 - {}^{A_0}/_{A_1})^{0.375} + (1 - {}^{A_0}/_{A_2})]^2 \quad \text{(A-5)}$$

where, A_0, A_1, A_2: cross-sectional areas (m^2), as defined in the figure.

A-2: Thick Sharp-Edged Orifice (0.015 L/D2.5 refer to Fig. A-2)

$$\zeta = 0.5 * (1 - {}^{A_0}/_{A_1})^{0.75} + (1 - {}^{A_0}/_{A_2})^2 + \tau * (1 - {}^{A_0}/_{A_1})^{0.375} * (1 - {}^{A_0}/_{A_2}) + f\,{}^{L}/_{D} \quad \text{(A-6)}$$

where, A_0, A_1, A_2: cross-sectional areas (m^2), as defined in the figure,

L,D: length (m) and diameter (m), as defined in the figure,

τ: defined as $\tau(\varphi, \iota) = (2.4 - \iota) * 10^{-\varphi}$,

φ: defined as

$\varphi(\iota) = 0.25 + 0.535 * \iota^8 / (0.05 + \iota^8)$,

ι: defined as ι=L/D, *and*

f: defined as in Eq. (A-3) or (A-4).

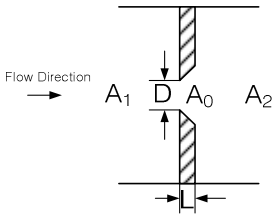

Fig. A-1 Thin sharp-edged orifice

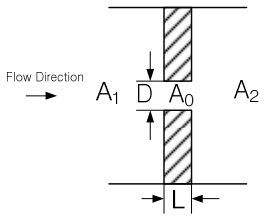

Fig. A-2 Thick sharp-edged orifice

A-3: Bell-Mouthed Pipe (or Nozzle refer to Fig. A-3)

$$\zeta = \zeta' * (1 - {}^{A_0}/_{A_1})^{0.75} + f\,{}^{(L-R)}/_{D} + (1 - {}^{A_0}/_{A_2})^2 \quad \text{(A-7)}$$

where, A_0, A_1, A_2: cross-sectional areas (m^2), as defined in the figure,

L,R,D: length (m), radius of curvature (m), and diameter (m), as defined in the figure,

f: defined as in Eq. (A-3) or (A-4), and

ζ': defined as $\zeta' = 0.03 + 0.47 * 10^{(-7.7 * R/D)}$.

A-4: Sharp-Edged Pipe (or Nozzle; refer to Fig. A-4)

$$\zeta = 0.5 * (1 - {}^{A_0}/_{A_1})^{0.75} + f\,{}^{L}/_{D} + (1 - {}^{A_0}/_{A_2})^2 \quad \text{(A-8)}$$

where, A_0, A_1, A_2: cross-sectional areas (m^2), as defined in the figure,

L,D: length (m) and diameter (m), as defined in the figure, and

f: defined as in Eq. (A-3) or (A-4).

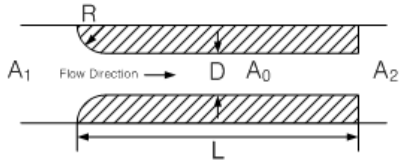

Fig. A-3 Bell-mouthed pipe (or nozzle)

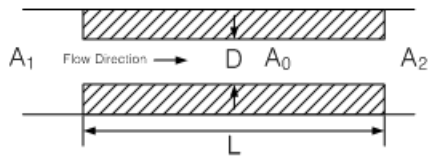

Fig. A-4 Sharp-edged pipe (or nozzle)